Report

Cell Reports

Functional Gene Correction for Cystic Fibrosis in Lung Epithelial Cells Generated from Patient iPSCs

Graphical Abstract

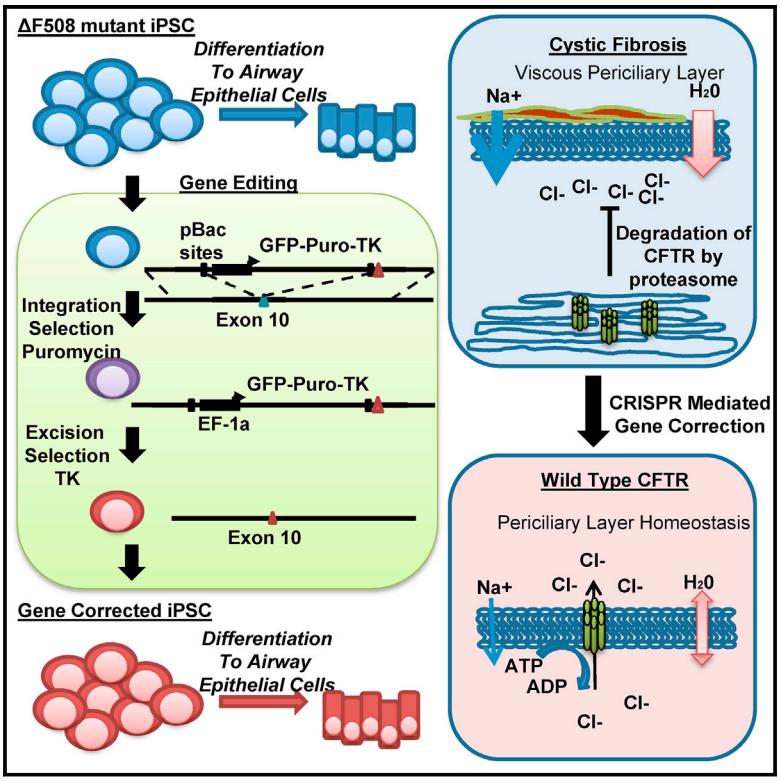

Highlights

- Generation of iPSCs from a CF patient homozygous for the common ΔF508 *CFTR* mutation
- CRISPR-based targeting of corrective sequences to endogenous *CFTR* gene in CF iPSCs
- Complete, efficient excision of selection markers by pBac transposase
- Differentiation to lung epithelial cells demonstrating functional correction of CFTR

Authors

Amy L. Firth, Tushar Menon, Gregory S. Parker, ..., Ajai Khanna, Fred H. Gage, Inder M. Verma

Correspondence

verma@salk.edu

In Brief

Firth et al. describe a robust in vitro human cellular model of CF with great therapeutic potential. A combination of CRISPR and pBac transposase technology allowed for efficient, footprint-free gene correction in CF iPSCs. Lung epithelial cells subsequently derived from corrected iPSCs demonstrated recovered function and expression of CFTR.

Firth et al., 2015, Cell Reports *12*, 1385–1390
September 1, 2015 ©2015 The Authors
http://dx.doi.org/10.1016/j.celrep.2015.07.062

Cell Reports
Report

Functional Gene Correction for Cystic Fibrosis in Lung Epithelial Cells Generated from Patient iPSCs

Amy L. Firth,[1,3] Tushar Menon,[1,3] Gregory S. Parker,[1] Susan J. Qualls,[1] Benjamin M. Lewis,[1] Eugene Ke,[1] Carl T. Dargitz,[1] Rebecca Wright,[1] Ajai Khanna,[2] Fred H. Gage,[1] and Inder M. Verma[1,*]
[1]The Salk Institute of Biological Studies, Laboratory of Genetics, 10010 North Torrey Pines Road, La Jolla, CA 92037, USA
[2]Center for Gut Rehabilitation and Transplantation, Digestive Disease Institute and Lerner College of Medicine, Cleveland Clinic, 9500 Euclid Avenue, Cleveland, OH 44195, USA
[3]Co-first author
*Correspondence: verma@salk.edu
http://dx.doi.org/10.1016/j.celrep.2015.07.062

SUMMARY

Lung disease is a major cause of death in the United States, with current therapeutic approaches serving only to manage symptoms. The most common chronic and life-threatening genetic disease of the lung is cystic fibrosis (CF) caused by mutations in the cystic fibrosis transmembrane regulator (*CFTR*). We have generated induced pluripotent stem cells (iPSCs) from CF patients carrying a homozygous deletion of F508 in the *CFTR* gene, which results in defective processing of *CFTR* to the cell membrane. This mutation was precisely corrected using CRISPR to target corrective sequences to the endogenous *CFTR* genomic locus, in combination with a completely excisable selection system, which significantly improved the efficiency of this correction. The corrected iPSCs were subsequently differentiated to mature airway epithelial cells where recovery of normal *CFTR* expression and function was demonstrated. This isogenic iPSC-based model system for CF could be adapted for the development of new therapeutic approaches.

INTRODUCTION

In cystic fibrosis (CF), a thick sticky mucus forms in the lungs impairing breathing and providing a rich environment for pathogens to flourish, leading to premature respiratory failure. It affects multiple organ systems leading to problems in the liver, pancreas, and small bowel. There has been a substantial increase in the knowledge of molecular and cellular mechanisms over the last two decades, which has translated to improvement in care and an increase in the average life expectancy from 14 years in 1980 to 37 years in 2012. The disease still severely impacts the quality of life with a significant shortening of life expectancy. Therefore, development of new therapeutic approaches is critical in the absence of a potential cure. The underlying cause, mutations in the cystic fibrosis transmembrane regulator (*CFTR*) gene, prevents the expression or function of this chloride transporter at the cell membrane (Rogan et al., 2011). Studying the disease has proven difficult due to the shortcomings of animal models. In the mouse *CFTR* knockout model, for example, an upregulation of calcium-activated chloride channels is sufficient to overcome the lack of functional *CFTR* (Boyd and Porteous, 2004). More recently, ferret and pig models of CF have been generated and thought to more closely replicate the human form of the disease (Rogers et al., 2008; Sun et al., 2010; Welsh et al., 2009). Studying the human disease still remains a challenge. There is a lack of availability of primary lung tissues and tissues from deceased CF patient lungs are inherently variable due to the differences in chronic infection and treatment regimens.

The ability to generate pluripotent stem cells from accessible tissues, such as skin, has opened the door for modeling human disease in a dish, increasing the potential for understanding the mechanisms of disease, testing novel therapeutic approaches, and developing cell therapies in a human system (Takahashi et al., 2007a, 2007b). Induced pluripotent stem cells (iPSCs), together with the recent explosion in genome-editing technologies, enable unprecedented capacity for patient-specific disease modeling, correction, and therapy. The latest tool in genome editing is called clustered, regularly interspaced, short palindromic repeats (CRISPR)-associated (Cas) systems, which is found naturally in the adaptive immune system of bacteria and archaea (Hale et al., 2012; Millen et al., 2012; Wiedenheft et al., 2012). The CRISPR system is essentially comprised of a ribonucleoprotein endonuclease, Cas9, that can catalyze double-strand cleavage of DNA in a sequence-specific manner defined by a guide RNA (gRNA) element complementary to the target DNA sequence. This simple two-component gene-targeting system has been co-opted for broader use by engineering synthetic gRNA hairpins to replace the bipartite bacterial RNA element (Jinek et al., 2012) and codon optimizing the bacterial Cas9 protein for optimized expression in higher eukaryotes (Cong et al., 2013; Mali et al., 2013). Recent work has shown that the CRISPR/Cas9 system can be used for efficient and multiplexed genome editing in a broad range of organisms, including bacteria (Jiang et al.,

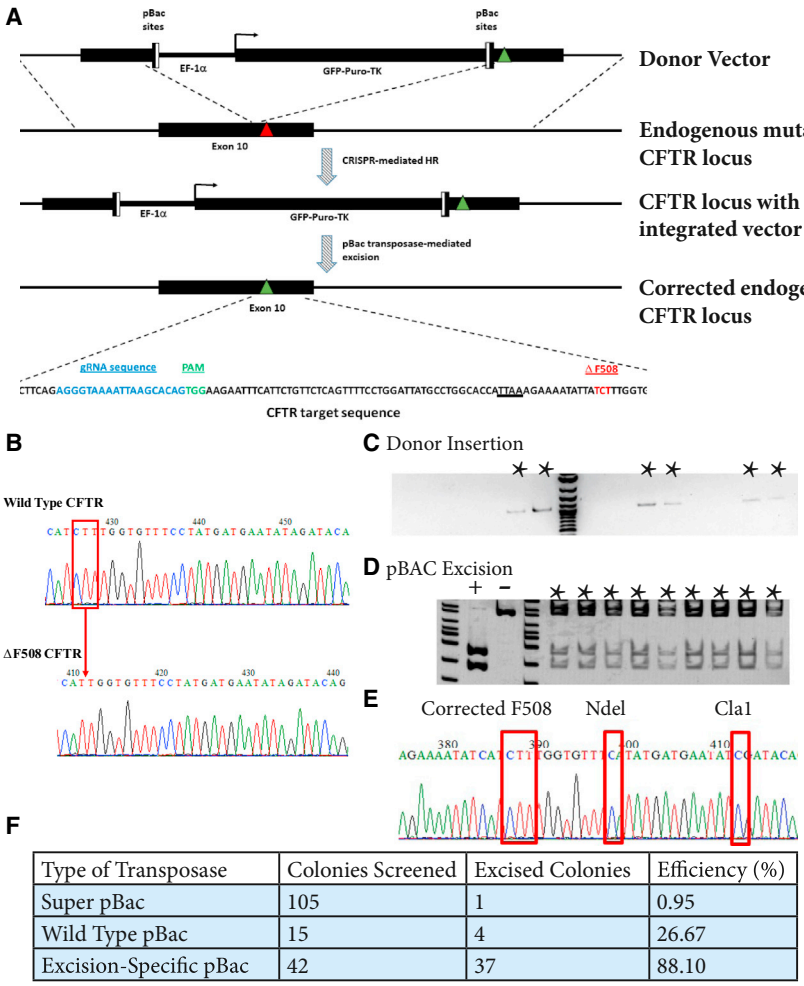

Type of Transposase	Colonies Screened	Excised Colonies	Efficiency (%)
Super pBac	105	1	0.95
Wild Type pBac	15	4	26.67
Excision-Specific pBac	42	37	88.10

Figure 1. Footprint-free CRISPR-Mediated Correction of CF iPSCs

(A) Schematic of strategy used for CRISPR-mediated correction of the *CFTR* ΔF508 mutation. Red triangle denotes the ΔF508 deletion (shown in red in the sequence at the bottom) and green triangles denote the correction of the deleted triplet of bases. The TTAA pBac recognition site is underlined. The actual *CFTR* target sequence is shown below with the gRNA target sequence in blue and the PAM in green.

(B) Sequencing analysis of the endogenous *CFTR* gene at the genomic locus of the ΔF508 mutation from wild-type and CF patient-derived iPSCs. The position of the CTT deletion in the mutant iPSCs as compared to the wild-type is indicated by the red box and arrow.

(C) Integration-specific PCR of puromycin-resistant single-cell clones of CF iPSCs after CRISPR treatment. Indicated clones contain the integrated selection cassette and corrective sequence in the correct position at the *CFTR* genomic locus.

(D) Screening by ClaI digest of a single-cell corrected clone after excision and negative selection of unexcised clones by ganciclovir. Indicated clones show precise and complete excision of the selection cassette from the endogenous *CFTR* genomic locus, leaving behind only the corrected F508 sequence and the intended silent mutations encoding the restrictions sites used for screening here.

(E) Sequencing analysis of corrected, excised clone shows the corrected ΔF508 mutation and adjacent silent mutations introduced in the endogenous *CFTR* gene.

(F) Excision screening was done with different variations of the pBac transposase.

2013), mice (Wang et al., 2013), zebrafish (Hwang et al., 2013), yeast (DiCarlo et al., 2013), *Xenopus tropicalis* (Nakayama et al., 2013), and human cells (Cho et al., 2013; Cong et al., 2013; Mali et al., 2013). The capability of Cas9 to mediate precise double-stranded breaks (DSBs) in the DNA genome opens the door to an infinite range of genome engineering possibilities.

RESULTS

Derivation of CF iPSCs and Strategy for Gene Correction of *CFTR* ΔF508

We obtained a skin biopsy from a CF patient organ donor; we isolated and expanded fibroblasts for reprogramming. The iPSCs were generated either by using a six-factor polycistronic lentivirus followed by successful excision using Cre-RNA (Firth et al., 2014) or by using four individual factor Sendai virus (Fusaki et al., 2009). All iPSC lines generated retained all the hallmarks of pluripotent stem cells (Figure S1). To correct the causative ΔF508 mutation in the patient-derived CF iPSCs, we developed a customized CRISPR system consisting of two components as follows: (1) a plasmid encoding the full-length Cas9 protein, codon optimized for optimal expression in human cells and driven by the stem cell-compatible eukaryotic transcription elongation factor 1 alpha 1 (*EEF1A1*) promoter; and (2) a separate plasmid containing a U6 promoter-driven gRNA hairpin cassette. The gRNA cassette was designed so that we could clone unique guide sequences into the RNA hairpin by using specifically designed primers containing the desired target guide sequences and PCR cloning into the vector backbone. The gRNAs were designed to target sequences in the vicinity of the ΔF508 mutation in the endogenous *CFTR* gene (Figure 1A). The patient-derived fibroblasts and iPSCs were confirmed to be homozygous for the phenylalanine deletion at position 508 (ΔF508) (Figure 1B). The functional activity of these gRNAs, in combination with our customized CRISPR system, was validated in HEK293T cells and in CF iPSCs by Surveyor assay (Figure S2A).

For targeting the ΔF508 mutation at its endogenous genomic locus, a donor vector was developed in order to achieve efficient, footprint-free correction of the *CFTR* gene (Figure 1A). The vector includes an *EEF1A1* promoter-driven GFP-Puro-TK cassette flanked with recognition sites for the piggyBac transposase along with the homology arms with the corrected *CFTR* sequence for integration into the endogenous genomic locus. Upon successful CRISPR-mediated integration into the genomic

target site, we can select for integration using puromycin and then seamlessly excise the selection cassette by expressing the pBac transposase (System Biosciences). This excision should proceed without leaving behind any genomic footprint from the donor vector other than the desired correction of the target ΔF508 mutation, as it uses a suitably placed TTAA pBac recognition site that occurs naturally within the target genomic sequence, as outlined in Figure 1A. We can then select against unexcised colonies in a subsequent round of clonal selection using ganciclovir sensitivity of clones expressing the unexcised thymidine kinase (TK) gene.

CRISPR-Mediated Gene Targeting of Endogenous *CFTR* in CF iPSCs

The Cas9 vector, *CFTR* gRNA vector, donor vector, and/or GFP were co-nucleofected in various combinations into CF iPSCs. Then, 48 hr after plating at a single-cell density, the colonies were treated with puromycin and the surviving colonies were selected and analyzed. The *CFTR* locus-specific segment of DNA was amplified using an integration-specific primer pair, with one primer contained within the selection cassette and the other outside the homology arm of the donor vector (Figure 1C). PCR products arising from clones screened with this combination of primers, spanning the junction between the target and insert, indicate that these puromycin-resistant clones contain the integrated selection cassette and corrective sequences in the correct location and orientation. Of the 36 clones picked and analyzed, six were positive for correct integration, at an overall efficiency of 16.7%. The sequence of the integration-specific product at the correct target locus in at least one allele of the endogenous *CFTR* gene in each of the positive clones was confirmed by sequencing.

Complete Excision of Selection Markers Using piggyBac Transposase

The selection cassette was subsequently excised using the piggyBac transposase system, which allows removal of the pBac site-flanked sequence without leaving behind any genomic footprint at the target site. Three variations of the piggyBac transposase (wild-type, integration-specific Super PiggyBac, or an excision-specific version from System Biosciences) were nucleofected into one of the integration-positive iPSC clones, to compare their relative efficiencies at excising the integrated cassette. The genomic DNA for each of the ganciclovir-resistant iPSC colonies was analyzed by PCR amplification of the *CFTR* locus and ClaI restriction enzyme digest of the amplicon (Figure 1D). The donor plasmid contained a silent mutation to introduce a ClaI site in close vicinity of the correction site. A number of corrected, excised clones were isolated, with nearly 90% efficiency when we used the excision-specific pBac transposase. A summary of excision experiments is provided in Figure 1F.

Analysis of Off-Target Effects of Genome-Editing Approach

Corrected, excised clones were verified by sequencing (Figure 1E) and one particular clone was then analyzed in detail for off-target effects of CRISPR by whole-exome sequencing. We compared observed mutations to predicted off-target sites using the CRISPR design tool (http://crispr.mit.edu/; Cong et al., 2013). No mutations (single nucleotide variants [SNVs], insertions and deletions) occurred within 300 bp of a predicted off-target site. After filtering, the predominant type of mutation was SNVs (80%) with the remainder being insertions and deletions at roughly the same proportion (Figure S2B). With regard to the length of these observed insertions and deletions, a heavy skew was observed to lengths that were <3 nt (Figure S2C). Given the type of mutations, short length of insertions and deletions, and lack of predicted off-target events, the acquired mutations were not due to the correction technology itself. Table S2 lists all the observed mutations derived from the whole-exome sequencing data. PCR analysis of genomic DNA of corrected clones, both before and after excision and using primers specific to the selection cassette, was negative, indicating there was no random integration of the selection cassette elsewhere in the genome (data not shown).

Recovery of *CFTR* Function in Airway Epithelial Cells Derived from iPSCs

Differentiation to proximal airway epithelial cells was carried out as previously described (Firth et al., 2014). Briefly, our mutant and gene-corrected CF iPSC lines were differentiated through definitive endoderm (DE), anterior foregut endoderm (AFE), and *NKX2.1* lung progenitors, and were matured in an air-liquid interface. All iPSC lines were capable of generating DE, as shown in Figure 2A by *FOXA2* staining, and maturing to lung epithelial cells with tight junctions after 48 days of differentiation, as indicated by ZO-1 staining occludin (red) in the lower images of Figure 2A. The qPCR analysis of key genes representing different stages of lung differentiation is shown in Figure 2B for wild-type, CF-mutant, and CF-corrected iPSCs. DE markers Forkhead box A2 (*FOXA2*), GATA-binding protein 6 (*GATA6*), and sex-determining region Y box 17 (*SOX17*) all increased by day 5 of differentiation. NK2 homeobox 1 (*NKX2.1*), one of the earliest transcription factors specifying lung, increased over the differentiation time course, as did club cell 10-kDa protein (CC10, club cells), keratin 5 (*KRT5*) and tumor protein 63 (*TP63*) (basal cells), Mucin 5AC (*MUC5AC*, goblet cells), and *CFTR* (functional epithelial cells).

We isolated epithelial cell adhesion molecule (*EPCAM*)-positive cells at day 48 of differentiation for analysis of *CFTR* currents by whole-cell patch clamp methods. In the mutant differentiated cells, no increase in *CFTR* chloride current was observed in response to a cocktail of forskolin, genistein, and isobutylmethyl xanthine (IBMX). In the CRISPR gene-corrected epithelial cells, half of the cells stably patched responded to stimulation, similar to our observations in wild-type iPSC-derived lung epithelial cells (Firth et al., 2014). The increase in current was blocked by specific *CFTR* inhibitor *CFTR*inh-172 (Figure 2C). Additionally, *CFTR* undergoes N-glycosylation, enabling conformational changes essential to its translocation to the cell membrane. *CFTR* contains two glycosylation sites that can be detected by gel electrophoresis of the protein. Core glycosylation produced a band of ~150 kDa (band A) and complex glycosylation produced a band of ~170 kDa (band B); ΔF508 mutant *CFTR* is unable to be glycosylated and only band A can be detected (Patrick et al., 2011). The western blot in Figure 2D shows the presence of

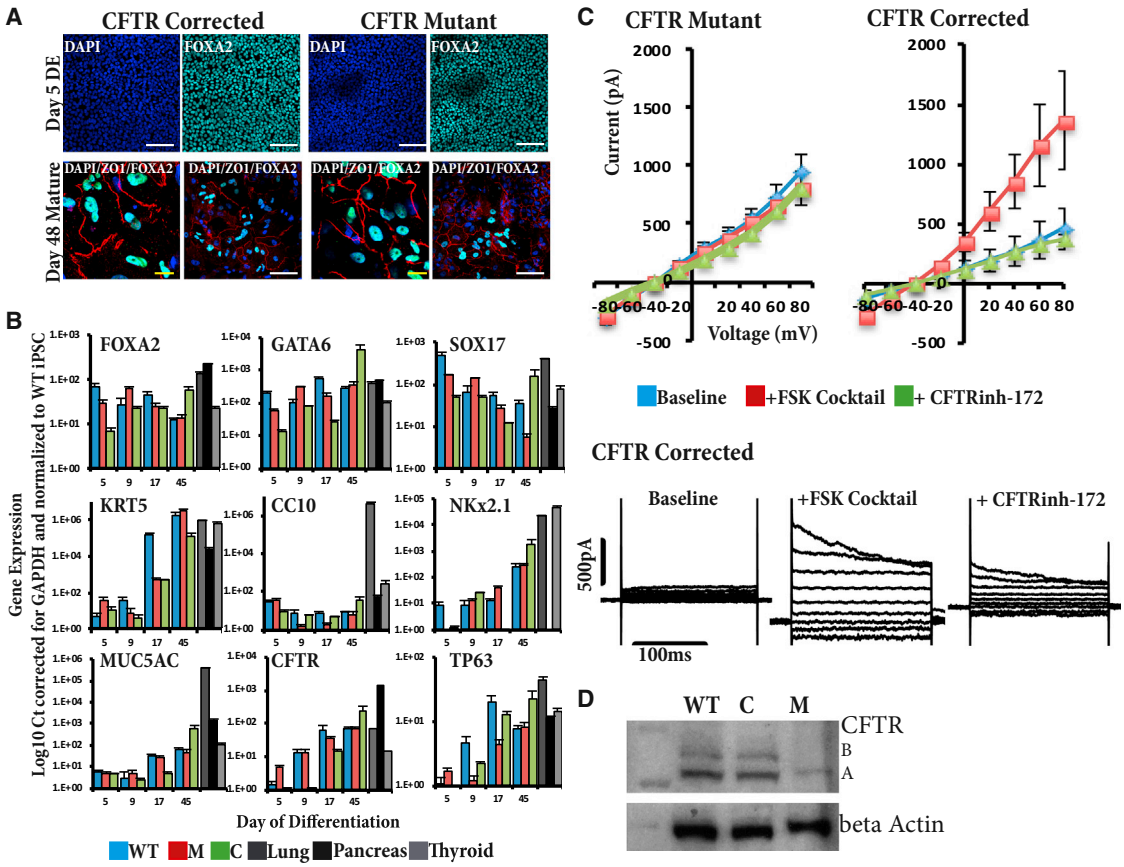

Figure 2. Generation of Functional Respiratory Epithelial Cells from CF Mutant and Gene-Corrected iPSCs

(A) Representative images show CF-corrected and CF-mutant iPSC differentiation to DE (day 5) with DAPI (blue) and *FOXA2* (cyan). Scale bars, 100 μm (white) and 20 μm (yellow).

(B) The mRNA expression of DE, AFE, and lung epithelial cell markers over the time course of differentiation for wild-type, CF-mutant, and CF-corrected iPSCs. Data are corrected for internal controls and normalized to wild-type iPSC cDNA (mean ± SEM, n = 6–15 from a minimum of three experimental replicates).

(C) Averaged current/voltage plots for baseline (blue), in presence of forskolin, genistein, and IBMX (pink) and with the addition of *CFTR*inh-172 (green). Data represented are mean ± SEM for zero of four patched mutant cells and three of eight patched gene-corrected cells. (Bottom) Representative current traces from one gene-corrected differentiated epithelial cell at baseline and in the presence of FSK cocktail and *CFTR*inh-172 (left to right); traces represent 20-mV increments from −80 to +80 mV.

(D) Western blot showing the presence of the membrane translocated and glycosylated protein in the wild-type and gene corrected cells (band B) and the unglycoslylated *CFTR* band in all three cell lines (band A). WT, wild-type; M, mutant; C, gene corrected.

the un-glycosylated and glycosylated bands in differentiated wild-type and gene-corrected iPSCs, but only the un-glycosylated band in the differentiated CF-mutant iPSCs.

DISCUSSION

While genomic correction of CF patient iPSCs recently has been demonstrated using zinc-finger nucleases (ZFNs) (Crane et al., 2015), this report now describes correction of iPSCs derived from a CF patient carrying the most commonly found homozygous ΔF508 mutation using CRISPR. CRISPR also recently has been used to correct *CFTR* in adult intestinal stem cells; however, these cells cannot be utilized to study the pathophysiology of CF in the lung (Schwank et al., 2013). Our footprint-free CRISPR-based approach is able to address some of the technical limitations regarding the persistence of a single LoxP site after CRE excision of the donor sequence and the use of integrating vector to generate the iPSCs (Crane et al., 2015), thus providing a more optimal approach when considering clinical applications. In addition, we observe a much-improved efficiency of genomic correction using our selection-based methodology with CRISPR, while completely eliminating any local genomic footprint in the endogenous *CFTR* gene.

Having such a footprint-free approach to gene editing has enabled us to precisely and efficiently edit a point mutation in the genome while leaving no genomic scar in patient cells. It is hoped that eventually this approach could be utilized as a cell therapy approach for patients with lung disease. A more immediate use for such cells would be for their utilization in research and drug development. Further refinement of the differentiation protocol will lead to effective in vitro isogenic models of human lung diseases like CF, which can be used to study mechanisms

of disease, screen for novel therapeutic approaches, and even clinically to identify responders to currently available therapeutic options.

EXPERIMENTAL PROCEDURES

Tissue used in this study was donated by organ donors/cadavers and Institutional Review Board exception was granted.

Nucleofection of iPSCs

Adherent cells were dissociated using Tryple (Gibco), centrifuged, and resuspended in TeSR containing 10 μM ROCK inhibitor, Y27632. Cells (1×10^6) were resuspended in 100 μl Lonza Nucleofection solution (according to the manufacturer's protocol). The following amounts of DNA were added: 2 μg Cas9, 2 μg gRNA, 5 μg PBHR, 2 μg pmaxGFP, and/or 2.5 μg PiggyBac Transposase in the required experimental combination. The samples were then nucleofected using the B-16 protocol on the device. After nucleofection, TeSR was added and cells transferred to a six-well Matrigel-coated plate. After 24–48 hr of incubation, the nucleofected iPSCs were split onto 10-cm mouse embryonic fibroblast (MEF) plates at single-cell density for colony screening or harvested for genomic DNA analysis.

Colony Isolation and Screening

After puromycin (1 μg/ml) or ganciclovir (3 μg/ml) treatment, colonies were mechanically passaged into a matrigel-coated 12-well plate in TeSR with ROCK inhibitor. Once the isolated iPSC clones were grown to the appropriate size, each well was split into duplicate 12-well matrigel plates. The cells were dissociated using trypsin, centrifuged at 1,000 rpm for 5 min, and resuspended in 1 ml TeSR with ROCK inhibitor. Two-thirds of each cell suspension was added to a matrigel plate for genomic DNA isolation, while the other third was carried to another matrigel plate designated for clonal maintenance and expansion. Genomic DNA was isolated as described in the Supplemental Experimental Procedures. To screen genomic DNA samples for integration of the corrective/selective sequences, the *CFTR* target locus was amplified by PCR, to yield an integration-specific product using one primer within the selection cassette and one outside the homology arm in the genomic sequence upstream of the integration site (F: CTTCCTCTGCTACCTCCTTTCC, R: CCGATAAAACA CATGCGTCA). For screening excised colonies, PCR products were digested with ClaI, a silent restriction site that was introduced via the targeting vector, at 37°C in an incubator for at least 1 hr. Digests were run on a 1% agarose gel and excised clones were identified by the presence of cleavage products of the expected sizes.

PiggyBac Transposase Nucleofection: Excision

Excision of the integrated selection cassette from corrected clones was done by overexpressing piggyBac transposase in clonal iPSC lines expressing puromycin resistance and sensitivity to ganciclovir. Various piggyBac transposase vectors (4 μg, System Biosciences) were nucleofected into 1×10^6 iPSCs using the Amaxa Nucleofector Device as described above, followed by selection with 3 μg/ml ganciclovir to eliminate unexcised cells.

Differentiation to Respiratory Epithelial Cells

Differentiation was carried out as previously described (Firth et al., 2014). Briefly, transwell inserts were coated with a combination of fibronectin (50 μg/ml), laminin (5 μg/ml), and collagen IV (60 mg/ml, Sigma-Aldrich). A single-cell suspension of iPSC was generated using Accutase. Then, 300,000 iPSCs were plated per 30-mm insert in TeSR with ROCK inhibitor for 24 hr. Differentiation to airway epithelial cells proceeded with media changes as detailed in Firth et al. (2014). Data were analyzed at day 42 of differentiation (day 28 of ALI). Methodology for immunofluorescence imaging is included in the Supplemental Experimental Procedures and antibodies are listed in Table S2.

Analysis of the Epithelial Differentiation

Immunocytochemistry was carried out on paraffin-embossed sections as previously detailed (Firth et al., 2014). RNA was isolated using the QIAGEN RNeasy kit as per the manufacturer's instructions and 500 ng RNA was reverse transcribed using a high-capacity cDNA kit (Applied Biosciences) as previously described (Firth et al., 2014). Real-time qPCR was carried out on the 7900HT Fast Real-Time PCR System in the Salk Functional Genomics Core facility, and data were analyzed using SDS2.3 and Microsoft Excel. Data are expressed as relative expression (ct) corrected for internal control GAPDH and normalized to iPSC ± SEM.

Western Blot

Protein was isolated from the samples using RIPA buffer with protease inhibitors for 30 min on ice. Protein lysate (40 μg) was loaded onto a 4%–12% Bis-Tris gel (Life Technologies) and run in MOPS buffer (Life Technologies). Protein was transferred to a nitrocellulose membrane The membrane was probed with mouse anti-human *CFTR*-570 (1:1,000) and anti-human β-actin (1:5,000).

Patch-Clamp Electrophysiology

Patch-clamp experiments were carried out as previously described (Firth et al., 2014). Briefly, the pipette (intracellular) solution contained the following (in mM): NaCl (5), $MgCl_2$ (2), CsCl (145), EGTA (10), HEPES (10), MgATP (5), and CsOH (to pH 7.2). The bath (extracellular) solution contained the following (in mM): $CaCl_2$ (2), NaCl (150), $MgCl_2$ (2), HEPES (10), and Tris HCl (to pH 7.4). Cells were held at a holding potential of −40 mV and 200-ms depolarizing steps in 20-mV increments from −80 to +80 mV were applied. The data were filtered at 3.3 kHz and digitized at 4 kHz. Cm and Rs were routinely compensated for. Pipette resistance was 2–4 MOhm. For *CFTR* activation, forskolin (10 μM), IBMX (100 μM), and genistein (50 μM) were added to the extracellular solution, and the cells were perfused for 5 min prior to recording. After *CFTR* activation, cells were perfused with *CFTR*-inh172 (3-[(3-trifluoromethyl) phenyl]-5-[(4-carboxyphenyl)methylene]-2-thioxo-4-thiazolidinone,10 μM) for 5 min prior to recording.

ACCESSION NUMBERS

The accession number for the whole-exome sequencing data reported in this paper is SRA: PRJNA291406.

SUPPLEMENTAL INFORMATION

Supplemental Information includes Supplemental Experimental Procedures, two figures, and two tables and can be found with this article online at http://dx.doi.org/10.1016/j.celrep.2015.07.062.

AUTHOR CONTRIBUTIONS

A.L.F. and T.M. generated the idea, designed the experiments, performed the experiments, analyzed data, and wrote the manuscript. G.S.P. assisted with the stem cell and gene correction experiments. S.J.Q. and C.T.D. assisted with all the stem cell experiments. B.M.L. assisted with the gene correction experiments. E.K. analyzed and presented data from the exome sequencing. R.W. performed the electrophysiology experiments. A.K. provided patient tissues for the experiments, academic input, and review of the manuscript. F.H.G. provided support and coordinated the electrophysiology experiments. I.M.V. designed and coordinated the research, provided support, and wrote the manuscript.

ACKNOWLEDGMENTS

We acknowledge Dr. Gerald M. Pao for valuable technical expertise and scientific discussions. Research reported in this article made use of the Waitt Advanced Biophotonics Center Core Facility (supported by the Waitt Foundation, NCI P30 CA014195-40 and NINDS P30 NS072031-03), the Flow Cytometry and Functional Genomics Core Facilities (supported by NCI P30 CA014195-40), and the Stem Cell Core Facility. T.M. was supported by a Pioneer Fund Postdoctoral Scholar Award. A.L.F. was supported by a California Institute for Regenerative Medicine (CIRM) Postdoctoral Training Fellowship TG2-01158. C.T.D. (2012), G.S.P. (2013), and B.M.L. (2014) were

supported by CIRM-Bridges Internship TB1-01175. I.M.V. is an American Cancer Society Professor of Molecular Biology and holds the Irwin and Joan Jacobs Chair in Exemplary Life Science. This work was supported in part by grants from the NIH (P30 CA014195-38, AI048034, and HL053670), CIRM (CL1-00500-1.2), Ipsen, Sanofi Aventis, the H.N. and Frances C. Berger Foundation, and The Leona M. and Harry B. Helmsley Charitable Trust grant 2012-PG-MED002. Lifesharing[R] of San Diego collaborated with tissue recovery.

Received: April 29, 2015
Revised: July 6, 2015
Accepted: July 29, 2015
Published: August 20, 2015

REFERENCES

Boyd, A.C., and Porteous, D.J. (2004). Revisiting the mouse lung model for CF. Gene Ther. *11*, 737–738.

Cho, S.W., Kim, S., Kim, J.M., and Kim, J.S. (2013). Targeted genome engineering in human cells with the Cas9 RNA-guided endonuclease. Nat. Biotechnol. *31*, 230–232.

Cong, L., Ran, F.A., Cox, D., Lin, S., Barretto, R., Habib, N., Hsu, P.D., Wu, X., Jiang, W., Marraffini, L.A., and Zhang, F. (2013). Multiplex genome engineering using CRISPR/Cas systems. Science *339*, 819–823.

Crane, A.M., Kramer, P., Bui, J.H., Chung, W.J., Li, X.S., Gonzalez-Garay, M.L., Hawkins, F., Liao, W., Mora, D., Choi, S., et al. (2015). Targeted correction and restored function of the CFTR gene in cystic fibrosis induced pluripotent stem cells. Stem Cell Reports *4*, 569–577.

DiCarlo, J.E., Norville, J.E., Mali, P., Rios, X., Aach, J., and Church, G.M. (2013). Genome engineering in Saccharomyces cerevisiae using CRISPR-Cas systems. Nucleic Acids Res. *41*, 4336–4343.

Firth, A.L., Dargitz, C.T., Qualls, S.J., Menon, T., Wright, R., Singer, O., Gage, F.H., Khanna, A., and Verma, I.M. (2014). Generation of multiciliated cells in functional airway epithelia from human induced pluripotent stem cells. Proc. Natl. Acad. Sci. USA *111*, E1723–E1730.

Fusaki, N., Ban, H., Nishiyama, A., Saeki, K., and Hasegawa, M. (2009). Efficient induction of transgene-free human pluripotent stem cells using a vector based on Sendai virus, an RNA virus that does not integrate into the host genome. Proc. Jpn. Acad., Ser. B, Phys. Biol. Sci. *85*, 348–362.

Hale, C.R., Majumdar, S., Elmore, J., Pfister, N., Compton, M., Olson, S., Resch, A.M., Glover, C.V., 3rd, Graveley, B.R., Terns, R.M., and Terns, M.P. (2012). Essential features and rational design of CRISPR RNAs that function with the Cas RAMP module complex to cleave RNAs. Mol. Cell *45*, 292–302.

Hwang, W.Y., Fu, Y., Reyon, D., Maeder, M.L., Tsai, S.Q., Sander, J.D., Peterson, R.T., Yeh, J.R., and Joung, J.K. (2013). Efficient genome editing in zebrafish using a CRISPR-Cas system. Nat. Biotechnol. *31*, 227–229.

Jiang, W., Bikard, D., Cox, D., Zhang, F., and Marraffini, L.A. (2013). RNA-guided editing of bacterial genomes using CRISPR-Cas systems. Nat. Biotechnol. *31*, 233–239.

Jinek, M., Chylinski, K., Fonfara, I., Hauer, M., Doudna, J.A., and Charpentier, E. (2012). A programmable dual-RNA-guided DNA endonuclease in adaptive bacterial immunity. Science *337*, 816–821.

Mali, P., Yang, L., Esvelt, K.M., Aach, J., Guell, M., DiCarlo, J.E., Norville, J.E., and Church, G.M. (2013). RNA-guided human genome engineering via Cas9. Science *339*, 823–826.

Millen, A.M., Horvath, P., Boyaval, P., and Romero, D.A. (2012). Mobile CRISPR/Cas-mediated bacteriophage resistance in Lactococcus lactis. PLoS ONE *7*, e51663.

Nakayama, T., Fish, M.B., Fisher, M., Oomen-Hajagos, J., Thomsen, G.H., and Grainger, R.M. (2013). Simple and efficient CRISPR/Cas9-mediated targeted mutagenesis in Xenopus tropicalis. Genesis *51*, 835–843.

Patrick, A.E., Karamyshev, A.L., Millen, L., and Thomas, P.J. (2011). Alteration of CFTR transmembrane span integration by disease-causing mutations. Mol. Biol. Cell *22*, 4461–4471.

Rogan, M.P., Stoltz, D.A., and Hornick, D.B. (2011). Cystic fibrosis transmembrane conductance regulator intracellular processing, trafficking, and opportunities for mutation-specific treatment. Chest *139*, 1480–1490.

Rogers, C.S., Stoltz, D.A., Meyerholz, D.K., Ostedgaard, L.S., Rokhlina, T., Taft, P.J., Rogan, M.P., Pezzulo, A.A., Karp, P.H., Itani, O.A., et al. (2008). Disruption of the CFTR gene produces a model of cystic fibrosis in newborn pigs. Science *321*, 1837–1841.

Schwank, G., Koo, B.K., Sasselli, V., Dekkers, J.F., Heo, I., Demircan, T., Sasaki, N., Boymans, S., Cuppen, E., van der Ent, C.K., et al. (2013). Functional repair of CFTR by CRISPR/Cas9 in intestinal stem cell organoids of cystic fibrosis patients. Cell Stem Cell *13*, 653–658.

Sun, X., Sui, H., Fisher, J.T., Yan, Z., Liu, X., Cho, H.J., Joo, N.S., Zhang, Y., Zhou, W., Yi, Y., et al. (2010). Disease phenotype of a ferret CFTR-knockout model of cystic fibrosis. J. Clin. Invest. *120*, 3149–3160.

Takahashi, K., Okita, K., Nakagawa, M., and Yamanaka, S. (2007a). Induction of pluripotent stem cells from fibroblast cultures. Nat. Protoc. *2*, 3081–3089.

Takahashi, K., Tanabe, K., Ohnuki, M., Narita, M., Ichisaka, T., Tomoda, K., and Yamanaka, S. (2007b). Induction of pluripotent stem cells from adult human fibroblasts by defined factors. Cell *131*, 861–872.

Wang, H., Yang, H., Shivalila, C.S., Dawlaty, M.M., Cheng, A.W., Zhang, F., and Jaenisch, R. (2013). One-step generation of mice carrying mutations in multiple genes by CRISPR/Cas-mediated genome engineering. Cell *153*, 910–918.

Welsh, M.J., Rogers, C.S., Stoltz, D.A., Meyerholz, D.K., and Prather, R.S. (2009). Development of a porcine model of cystic fibrosis. Trans. Am. Clin. Climatol. Assoc. *120*, 149–162.

Wiedenheft, B., Sternberg, S.H., and Doudna, J.A. (2012). RNA-guided genetic silencing systems in bacteria and archaea. Nature *482*, 331–338.